Cell Metabolism

Supplemental Information

GDF11 Increases with Age and Inhibits Skeletal Muscle Regeneration

Marc A. Egerman, Samuel M. Cadena, Jason A. Gilbert, Angelika Meyer, Hallie N. Nelson, Susanne E. Swalley, Carolyn Mallozzi, Carsten Jacobi, Lori L. Jennings, Ieuan Clay, Gaëlle Laurent, Shenglin Ma, Sophie Brachat, Estelle Lach-Trifilieff, Tea Shavlakadze, Anne-Ulrike Trendelenburg, Andrew S. Brack, David J. Glass

SUPPLEMENTAL EXPERIMENTAL PROCEDURES

RNAseq analysis

Briefly, we aligned 2X76 bp pair-end reads to rat genome rn5 using STAR [1] with default parameters. About 21 million reads were mapped for each sample. We counted the number of reads per million at 10 bp resolution throughout the genome, and then averaged the normalized read counts across all exons of each Refseq gene to measure its expression level. In order to model aging-regulated expression changes, we standardized the expression levels across all samples for each gene, and fitted 4 arameter logistic curves to the standardized expression level.

qPCR analysis

RNA from rat gastrocnemius muscle was isolated using a RNEasy Mini Kit (Qiagen), per the manufacturer's protocol. cDNA synthesis was performed using a High Capacity cDNA Reverse Transcription kit (Applied Biosystems). cDNA was then used for quantitative PCR (qPCR) using an ABI Prism 7900 sequence detection system in combination with Taqman® fast PCR Master Mix (Applied Biosystems) to confirm findings from RNAseq study. The Taqman probes for myostatin (Rn00569683_m1) and Gdf11 (Rn01756258_m1) were purchased from Applied Biosystems. The PCR conditions consisted in one cycle of denaturation at 95ºC for 20 sec and 40 cycles of amplification consisting of a denaturation step at 95ºC for 1 sec and annealing/elongation step at 60ºC for 20 sec. Transcript levels were normalized to the housekeeping gene TBP in the same preparation, and the fold change relative to young samples was calculated as $2^{-\Delta\Delta CT}$.

Immunostaining

Cells were fixed with 4% paraformaldehyde for 15 minutes at room temperature then permeabilized with 0.5% Triton in PBS for 5 minutes. Nonspecific binding was blocked with normal goat serum (Invitrogen) for 20 minutes followed by incubation overnight at 4ºC with anti-MyHC diluted in PBS. Cells were then incubated with Alexa Fluor® 488 F (AB') and DAPI (Invitrogen) diluted in PBS for 1-3 hours with constant shaking. For long-term storage, ProLong Gold anti-fade reagent (Invitrogen) was subsequently added. Fixed muscle sections were stained with anti-Pax7, anti-lamin, and DAPI as described previously (Chakkalakal et al., 2014).

Imaging

HSkMDC cellular images were acquired using fluorescence microscopy (Cellomics ArrayScan) to assess effects of molecules on muscle differentiation. Using HSC Studio, DAPI stained nuclei were demarcated and a mask was generated 2 pixels outside of the nuclei boundary. The intensity of MyHC staining was quantified within the mask, and MyHC negative and positive cells were analyzed to establish a threshold used to determine MyHC positive nuclei relative to total nuclei (%MyHC positive nuclei). Twelve 10x fields were analyzed per well.

Reporter gene assays.

HEK293T cells stably transfected with the TGF-ß responsive reporter gene construct CAGA12-luc cloned into the reporter construct pGL3 (Promega) were kindly provided by C. Lu (Developmental and Molecular Pathways, Novartis Pharma AG). Reporter gene

activity was measured using Brite Lite Plus (Perkin Elmer) and chemiluminescence was read using a Spectramax M5 (Molecular Devices).

Microarray Study

Expression levels of mRNA were measured by microarray analysis of human primary muscle cells 24 hours after stimulation with 300 ng/mL of Myostatin, GDF11 and control (vehicle alone). Normalized total RNA samples (50 ng/µL) were supplied to the Genome Array Lab for reverse transcription, labeling and hybridization using an Affymetrix GeneChip Human Genome U133 Plus 2.0 Array (HG-U133_Plus_2). The experiment was performed in quadruplicate. Fold changes (FCs) and adjusted p-values were calculated between control samples and GDF11 or Myostatin stimulated samples. Fold change represents the mean value of four independent hybridizations to Affymetrix microarrays, HG-U133_Plus_2 (Complete coverage of the Human Genome U133 Set plus 6,500 additional genes for analysis of over 47,000 transcripts). Gene expression levels (based on RMA algorithm http://www.ncbi.nlm.nih.gov/pubmed/12925520) were calculated in R using the Bioconductor package affycore tools and affyio packages. QC was performed using the bioconductor package arrayQualityMetrics (Kaufmann and Huber, 2010) and principal component analysis. Lists of differentially expressed probe sets were produced with fold change and LIMMA t-test p-value calculation using the bioconductor packages limma, reshape and plyr (Wickham, 2011), using a factorial design approach (Smyth, 2005) to extract the relevant contrasts. P values were adjusted for multiple testing correction using the Nejamini and Horberg method. Annotation data for probes was obtained using the bioconductor packages “AnnotationDbi” and “hgu133plus2.db”.

Probesets with an absolute fold change of 2 and above and an adjusted p-value below 0.01 (Benjamini and Hochberg multiple testing correction) were considered regulated. The heat map was generated for genes regulated in at least one of the treatment (243 genes, 356 probesets) by UPGMA hierarchical clustering using Euclidian distance in Spotfire; 300 ng/mL dose. Data has been submitted to Gene expression Omnibus (GSE67326).

Satellite cell isolation and culture.

Satellite cells from adult (4 month) and aged (24 month) mice were isolated as described previously (Chakkalakal et al., 2014). Cells were collected based on the following cell surface markers: Lin- (CD45-,CD31-,Sca1-), Inta7+, VCAM+,PI-. Live cells (200 per well) were plated directly into ECM coated-96-well plates and maintained in growth media (20% horse serum diluted in DMEM) for three days, and then fixed. Cultures were supplemented daily with fresh GDF11 or vehicle. The wells were divided in sets of triplicates of control, low (15 ng/mL), and high (50 ng/mL) concentration of GDF11 (R&D systems) treatment. All cultures were stained for Pax7, and either MyoD, or Myogenin as described previously (Shea et al., 2010; Chakkalakal et al., 2014).

Regeneration model in vivo

All procedures involving animals were approved by the Institutional Animal Care and Use Committee of the Novartis Institutes for Biomedical Research, Cambridge, MA, USA. Four (Jackson Laboratories, Bar Harbor, Maine) and twenty-three month old male C57BL/6J mice (Janvier Labs, France) were housed individually with environmental enrichment in a temperature (22°C) and humidity-controlled (43%) room. Mice were maintained on a 12-h light-dark cycle and provided food (5053, PicoLab Rodent Diet 20; LabDiets) and water ad libitum. They were acclimated to the facility for ~7 days and then

age groups were weight-matched into experimental groups to receive daily intraperitoneal injections of GDF11 (0.1 or 0.3 mg/kg) or Vehicle (0.8 mM HCl in PBS) for the durations indicated. On the day of muscle injury mice were anesthetized by inhalation of 2-3% isoflurane in oxygen, legs shaved from ankle to knee and cleaned with 70% ethanol. The mid-belly of the tibialis anterior (TA) muscle was injected through the skin with 25 μl of cobra venom (0.12 mg/ml; ~97% cardiotoxin; CTX) from *Naja Melanoleuca* (Sigma-Aldrich) dissolved in sterile PBS. This concentration and volume of cobra venom typically induces 60-70% damage across the TA muscle mid-belly. After injection, animals were kept on a heating pad until recovery and returned to home cage.

Histology

Tibialis anterior muscles were harvested and snap frozen in liquid nitrogen cooled isopentane. Muscles were bisected at the mid-belly and 10 μm sections taken. For gross morphological analysis sections were H&E stained and for measurements of fiber cross-sectional area sections were stained for laminin and nuclei visualized by Hoechst 33342 (Life Technologies). Briefly, sections were blocked in 5% goat serum in PBS and incubated in rabbit anti-laminin (Sigma) diluted in 1:100 in blocking solution. Sections were then incubated in goat anti-rabbit secondary antibody conjugated to Alexa 488 (Life Technologies) diluted 1:200 in blocking solution. Whole stained sections were scanned on an Olympus VS120 fluorescent slide scanner. To ensure that the degree of CTX induced injury was consistent between treatment groups the area of regeneration was quantified in images of H&E stained sections. Samples with areas of regeneration (as determined by centralized nuclei) less than 50% were excluded from the analysis. Further,

samples with areas of regeneration less than or greater than two standard deviations of the combined mean of both experimental groups were also excluded from analysis.

Pharmacokinetic Study

4 month old C57BL/6 mice (Jackson Laboratories, Bar Harbor, Maine) received a single intraperitoneal injection of GDF11 at 0.1 mg/kg or Vehicle (0.8 mM HCl in PBS) and serial bled at the time points indicated.

Single muscle fiber isolation

Single muscle fibers were prepared as previously described (Shea et al., 2010). In brief single muscle fibers were digested in 0.2% collagenase type 1 (Worthington Biochemical Corporation) for 60 minutes. Muscles were then triturated to obtain single full-length muscle fibers. Fibers were cultured in 6-well plates for 3 days in DMEM with 10% horse serum, supplemented with GDF11 (50 ng/mL) or diluent daily.

Automated microscopy cell analysis.

Images of satellite cells were collected using the Nikon Eclipse Ti microscope. To image the whole well, 72 images at 10x magnification were collected without stitching to capture an image of almost the entire well. The objects (cells) per well were identified based on DAPI intensity, where the background (non-cell) was subtracted from each channel. Images were then processed using NIS Elements Advanced software. Using the perform measurement tool, the individual object (cell) intensities for each channel were generated. The intensities were sorted based on circularity, size, and area to exclude non-cells detected by the software.

Statistical Analysis

All in vivo data are presented as means ± SE. Mean muscle fiber cross-sectional area data were analyzed using non-paired two sample t-test and differences were considered statistically significant when the two-tailed P-value was ≤ 0.05.

All in vitro data are presented as means ± SE, unless otherwise indicated. Data were analyzed using non-paired two sample t-test and differences were considered statistically significant when the two-tailed P-value was ≤ 0.05.

SUPPLEMENTARY REFERENCES

Bernet JD, Doles JD, Hall JK, Kelly Tanaka K, Carter TA, Olwin BB (2014) p38 MAPK signaling underlies a cell-autonomous loss of stem cell self-renewal in skeletal muscle of aged mice. Nature Med., *20*, 265-71

Brack AS, Conboy MJ, Roy S, Lee M, Kuo CJ, Keller C, Rando TA (2007) Increased Wnt signaling during aging alters muscle stem cell fate and increases fibrosis. Science, *317*,807-10.

Chakkalakal JV, Christensen J, Xiang W, Tierney MT, Boscolo FS, Sacco A, Brack AS (2014) Early forming label-retaining muscle stem cells require p27kip1 for maintenance of the primitive state. Development, *141*, 1649-59.

Conboy, I.M., Conboy, M.J., Smythe, G.M. Rando, T.A. (2003) Notch-mediated restoration of regenerative potential to aged muscle. Science. *302*, 1575-7.

Conboy, I.M., Conboy, M.J., Wagers, A.J., Girma, E.R., Weissman, I.L., Rando, T.A. (2005) Rejuvenation of aged progenitor cells by exposure to a young systemic environment. Nature. *433*, 760-4.

Cosgrove BD, Gilbert PM, Porpiglia E, Mourkioti F, Lee SP, Corbel SY, Llewellyn ME, Delp SL, Blau HM. (2014) Rejuvenation of the muscle stem cell population restores strength to injured aged muscles. *20,* 255-64.

Dobin A et al. STAR: ultrafast universal RNA-seq aligner. Bioinformatics. 2013 Jan 1;29(1):15-21. doi: 10.1093/bioinformatics/bts635. Epub 2012 Oct 25.

Lee, S.-J., Reed, L.A., Davies, M.V., Girgenrath, S., Goad, M.E.P., Tomkinson, K.N., Wright, J.F., Barker, C., Ehrmantraut, G., Holmstrom, J., et al. (2005). Regulation of muscle growth by multiple ligands signaling through activin type II receptors. Proc Natl Acad Sci USA *102*, 18117-18122.

McCroskery S, Thomas M, Maxwell L, Sharma M, Kambadur R (2003) Myostatin negatively regulates satellite cell activation and self-renewal. J Cell Biol. *162*,1135-47.

McPherron, A., Huynh, T., and Lee, S.-J. (2009). Redundancy of myostatin and growth/differentiation factor 11 function. BMC Developmental Biology *9*, 24.

Relaix, F., Zammit, P.S. (2012) Satellite cells are essential for skeletal muscle regeneration: the cell on the edge returns centre stage. Development. Aug;139(16):2845-56.

Shea KL, Xiang W, LaPorta VS, Licht JD, Keller C, Basson MA, Brack AS. (2010 Sprouty1 regulates reversible quiescence of a self-renewing adult muscle stem cell pool during regeneration. Cell Stem Cell. *6,*117-29.

Sousa-Victor P, Gutarra S, García-Prat L, Rodriguez-Ubreva J, Ortet L, Ruiz-Bonilla V, Jardí M, Ballestar E, González S, Serrano AL, Perdiguero E, Muñoz-Cánoves P (2014)

Geriatric muscle stem cells switch reversible quiescence into senescence. Nature, *506*, 316-21.

Supplemental Figure Legends

Supplemental Figure 1, Related to Figure 1.

Prior reagents used to measure GDF11 are not specific, but show that the combination of GDF11 and Myostatin increases with age. Specific methods show GDF11 levels increase with age

A. Western analysis on sera from young and old mice.

Sera from three different young animals (4 month old; 1, 2, 3,) and three different old animals (23 month old; 5, 6, 7) were tested in a Western analysis for myostatin/GDF11 levels. As usual the dimer band was not fully denatured to monomer. Ponceau S staining (lower blot) demonstrates equivalent loading of each lane.

B. Western analysis on plasma from mouse injected with recombinant GDF11.

Plasma from a young mouse that received an intraperitoneal injection of 0.1 mg/kg recombinant GDF11 was tested via Western analysis. Sequential bleeds were taken 1, 4, 8, 24, and 48 hours post-injection. Densitometry quantifications (relative to 0 hour) are shown below. Injection of GDF11 causes an increase in detected sera GDF11. Recombinant GDF11 is shown on the left.

C. qPCR verification on skeletal muscle from young and old rats .

RNA from gastrocnemius muscles of young (6 month) and old (24 month) rats (n=8 in both groups) was processed for qPCR. Shown are the analyses of myostatin and Gdf11 mRNA levels normalized to TBP, with data expressed as relative gene expression (compared to the young group; blue bars). Shown are mean ± SE, with p value < 0.005 (**).

Supplemental Figure 2, related to Figure 1E and 1F. New GDF-11 specific Immunoassay

A. Specificity of the ECL immunoassay to GDF11 and Myostatin.

The ECL immunoassay is specific to GDF11 and is not found to cross-react with Myostatin. Myostatin or GDF11 was spiked into buffer at the concentrations listed in the table. Each bar represents the measured GDF11 concentration using the ECL immunoassay. The dotted lines represent 1.0 ng/mL and 10 ng/mL of GDF11. Buffer samples spiked with 1.0 or 10 ng/mL of Myostatin were both below the limit of quantification, and are reported at the lower limit of quantification (LLOQ) of the assay (0.137 ng/mL). Buffer samples spiked with 1.0 ng/mL GDF11 and either 0.0, 1.0 or 10 ng/mL Myostatin (red bars) had measured concentrations of 1.0 ng/mL (+/- 10%). Buffer samples spiked with 10 ng/mL GDF11 and either 0.0, 1.0 or 10 ng/mL Myostatin (blue bars) had measured concentrations of 10.0 ng/mL (+/- 10%).

B. Western analysis to determine specificity of R&D antibody on Myostatin versus GDF11.

A concentration gradient of recombinant myostatin and GDF11, ranging from 6.25 ng to 100 ng, was tested via Western analysis. The GDF11 antibody was found to not cross-react to myostatin. Ponceau S staining (*right*) included to ensure equivalent loading.

C. Dilution linearity and recovery of spiked human serum samples

9 human serum samples were spiked with 8 ng/mL of GDF11, serially diluted at 1:2, 1:4, 1:8, and 1:16 dilutions and measured GDF11 with the ECL immunoassay.

Selectivity (left): The concentration of GDF11 back-calculated at a 1:2 dilution was compared between the 8 ng/mL spiked sample (red bars) and its respective un-spiked sample (blue bars). The LLOQ of the assay (0.274 ng/mL) is represented by the dotted line. The endogenous level of samples 1, 5 and 7 were below the LLOQ of the assay. All human samples showed an increase in measured GDF11 when spiked with 8 ng/mL of recombinant material, with recoveries ranging from 19.7 to 46.1%. The % recovery of the sample was calculated using the following formula: ((measured concentration - endogenous concentration)/(8 ng/mL spike))*100.

Linearity (right): The back-calculated concentration of all the dilutions for each sample is shown on the graph. The LLOQ of the assay (0.274 ng/mL, considering 1:2 dilution factor) is represented by the dotted line. Two samples were excluded due to a high

concentration CV (>25%) between the two replicates. The measurement of GDF11 in human serum shows linearity with serial dilutions.

Supplemental Figure 3, Related to Figure 2.

Western analysis to determine Myostatin vs. GDF11 activation of downstream non-SMAD signaling

Murine C2C12 myotubes (day 4) were stimulated with vehicle (UNT), as a negative control, or with myostatin or GDF11, as indicated. Both proteins activated the MAPK signaling pathway, as indicated by the stimulation of p38 (*top*) and ERK (*below*).

Supplementary Figure 4, Related to Figure 4.

GDF11 does not improve regeneration in vivo in aged mice.

Tibialis anterior muscle was induced to regenerate after a cardiotoxin-induced injury in Vehicle or GDF11 treated aged mice. (**A**) Tibialis anterior muscle sections stained for H&E showed that there were no changes in gross morphology between treatment groups. (**B**) GDF11 treatment did not alter fiber cross-sectional area frequency distributions or (**C**) mean fiber areas in CTX injured muscles; indicating no improvement in muscle regeneration with GDF11 treatment in aged mice

Supplementary Figure 5, Related to Figure 5.

GDF11 does not impact myogenic lineage progression of adult and aged satellite cells.

A) Representative image of regenerating skeletal muscle section sectioned with anti-Pax7 (red), anti-Laminin (green) and DAPI (blue). B) Histogram shows the number of Pax7+ cells in regenerating (7 days post injury) vehicle and GDF11 treated aged mice showing there was no change in SC numbers between treatment groups. N=3 mice per treatment group. Data expressed as mean +/- SE. Histograms show (C) percentage and (D) fluorescence intensity of Pax7 (top), MyoD (middle), or Myogenin (lower) cells for adult and aged SCs, after 3 days of GDF11 (15ng/ml, low or 50ng/ml, high) or vehicle treatment in culture (n=1645-2185 cells, performed in triplicate). Data are represented as mean +/- SD. Cultures were were statistically analyzed by Kruskall Wallis non-parametric test with Dunn's post hoc test with no significant differences concluded ($p<0.05$).

Supplemental Figure 1

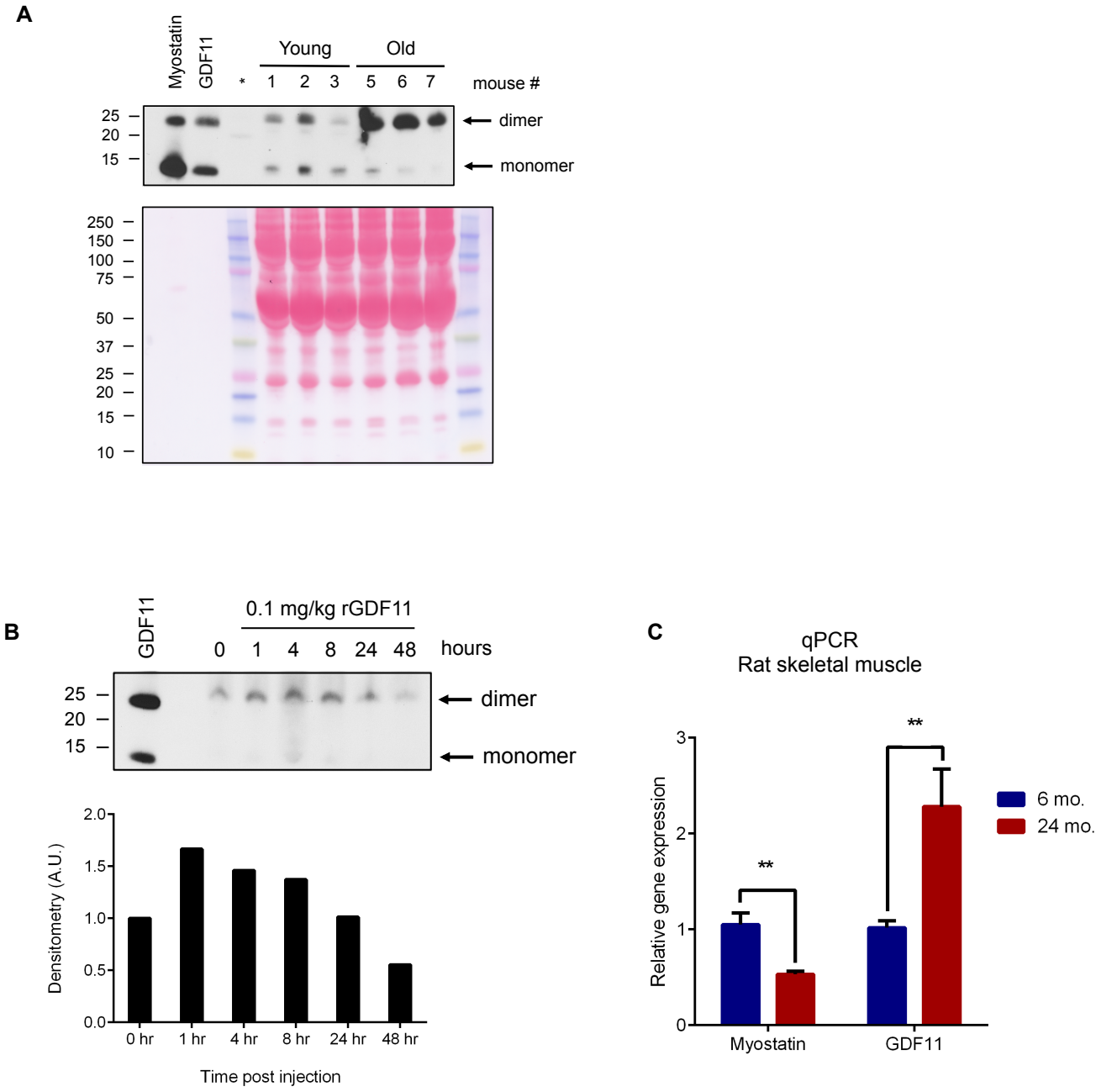

Supplemental Figure 2

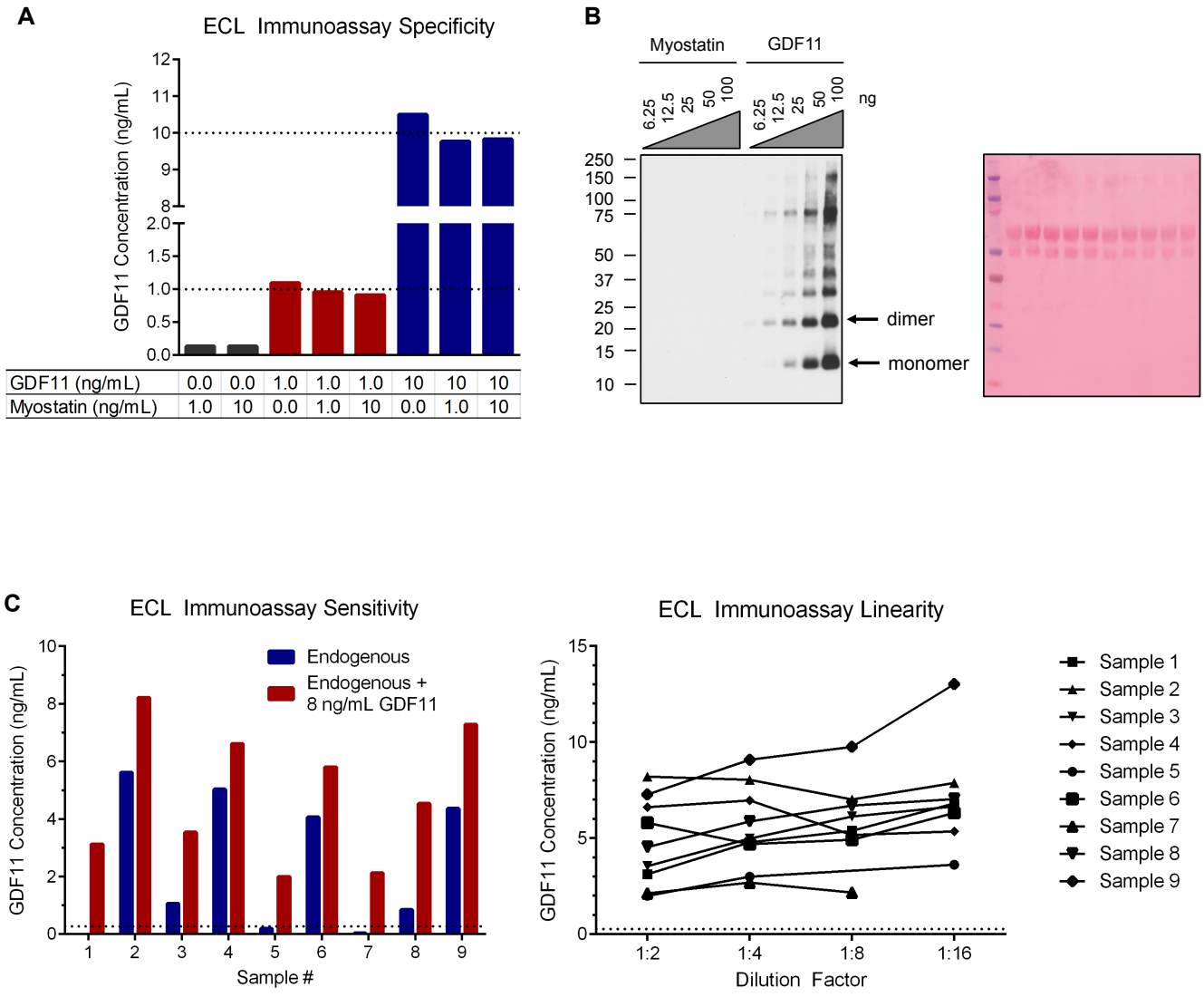

Supplemental Figure 3

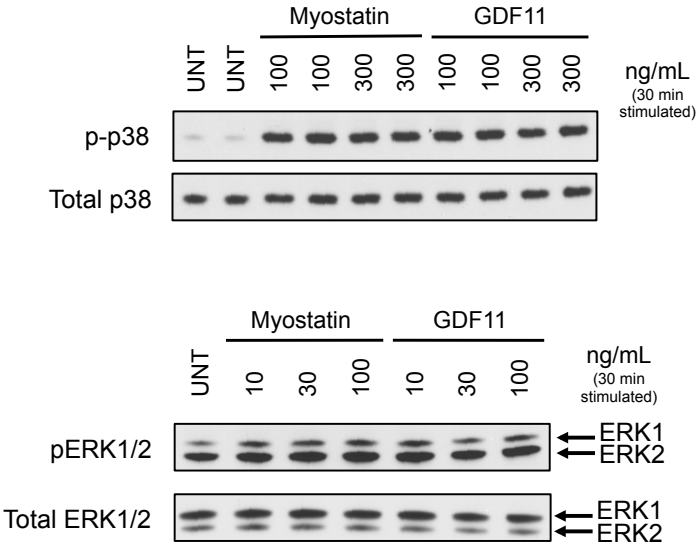

Supplemental Figure 4

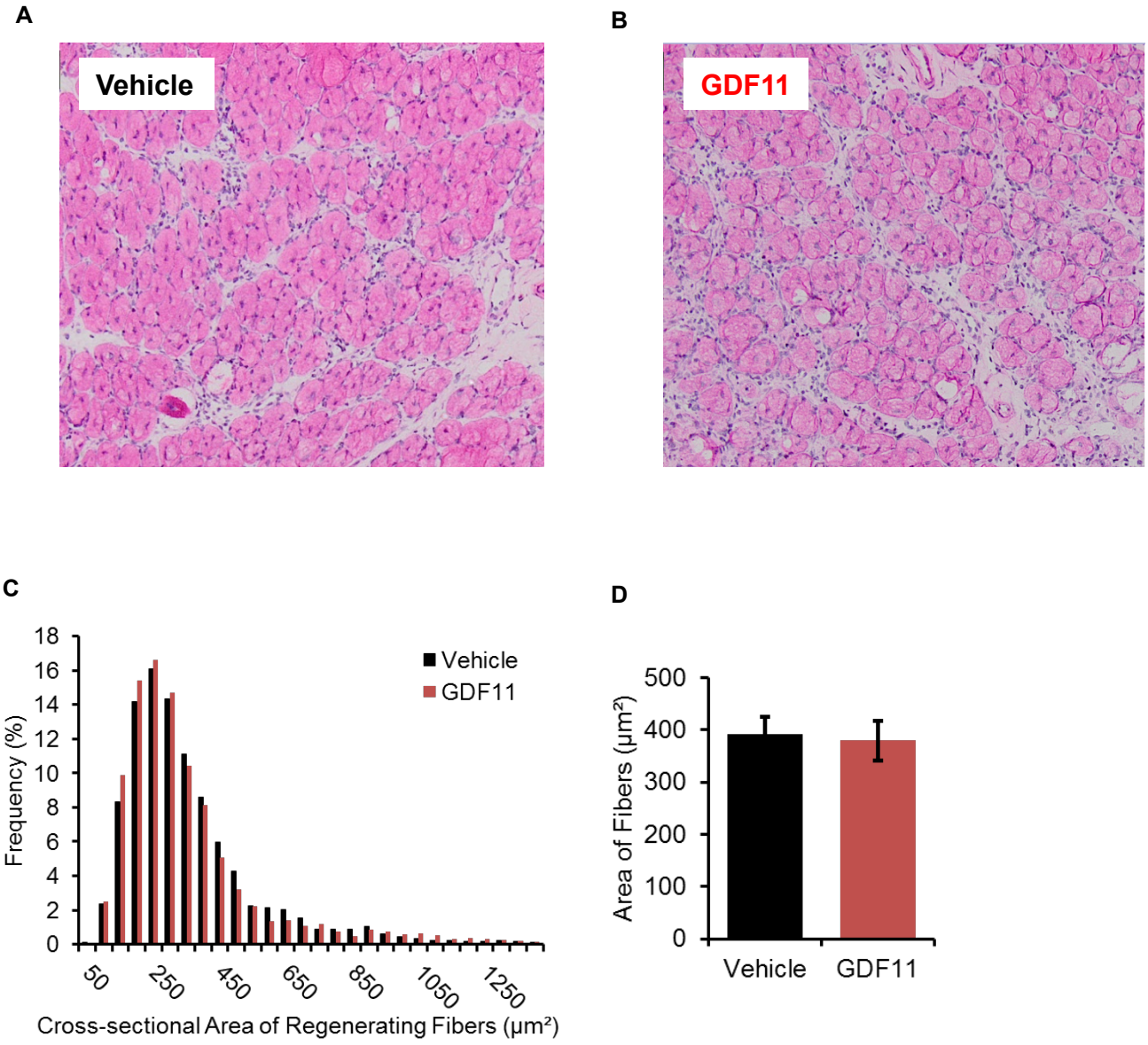

Supplemental Figure 5